Karel Vacek; Petr Sváček

On finite element approximation of fluid structure interaction by Taylor-Hood and Scott-Vogelius elements

In: Jan Chleboun and Pavel Kůs and Jan Papež and Miroslav Rozložník and Karel Segeth and Jakub Šístek (eds.): Programs and Algorithms of Numerical Mathematics, Proceedings of Seminar. Jablonec nad Nisou, June 19-24, 2022. Institute of Mathematics CAS, Prague, 2023. pp. 259–268.

Persistent URL: http://dml.cz/dmlcz/703206

Programs and Algorithms of Numerical Mathematics 21
J. Chleboun, P. Kůs, J. Papež, M. Rozložník, K. Segeth, J. Šístek (Eds.)
Institute of Mathematics CAS, Prague 2023

ON FINITE ELEMENT APPROXIMATION OF FLUID STRUCTURE INTERACTION BY TAYLOR–HOOD AND SCOTT-VOGELIUS ELEMENTS

Karel Vacek[1], Petr Sváček[2]

[1] Institute of Mathematics of the Czech Academy of Sciences,
Žitná 25, Prague 1
[2] Czech Technical University, Department of Technical Mathematics,
Karlovo náměstí 13, 121 35 Praha 2
karel.vacek@fs.cvut.cz, petr.svacek@fs.cvut.cz

Abstract: This paper focuses on mathematical modeling and finite element simulation of fluid-structure interaction problems. A simplified problem of two-dimensional incompressible fluid flow interacting with a rigid structure, whose motion is described with one degree of freedom, is considered. The problem is mathematically described and numerically approximated using the finite element method. Two possibilities, namely Taylor-Hood and Scott-Vogelius elements are presented and implemented. Finally, numerical results of the flow around the cylinder are shown and compared with the reference data.

Keywords: finite element method, FSI problem, ALE method, Taylor-Hood element, Scott-Vogelius element

MSC: 65N15, 65M15, 65F08

1. Introduction

The numerical approximations of the fluid-structure interaction play an important role in many areas of science and engineering, such as the flutter of aircraft wings, flow around wind turbine blades and hydrodynamics compressors. Although in this contribution simpler case of incompressible fluid flow is considered, there are a lot of numerical difficulties to be addressed as treatment of the incompressibility constraint, treatment of the nonlinear convective term, dominating convective term, etc., see e.g. [13], [12], [2]. Moreover, the time change of the computational fluid domain needs to be included. Here we use the well-known arbitrary Lagrangian-Eulerian (ALE) method due to it straightforward manner.

This paper focuses on the finite element method approximation of the Navier-Stokes equations. There are many available strategies, see e.g. [7], [6], but we will further deal only with finite elements which satisfy the Babuška-Brezzi (BB) inf-sup condition. The fulfillment of BB condition guarantees stability of the numerical

DOI: 10.21136/panm.2022.24

scheme, for an overview of such elements, see [7]. Here, we compare two of them. The first one is the well-known Taylor-Hood (TH) finite element (continuous piecewise quadratic velocities and continuous piecewise linear pressures) which satisfies the inf-sup condition only discretely. The second element is the Scott-Vogelius (SV) finite element, i.e. continuous piecewise quadratic velocities and discontinuous piecewise linear pressures, see [3], [6]. In order to satisfy the BB condition, the finite element (FE) approximation space is constructed over a barycentric refinement of an admissible triangulation, see [4]. By choosing this element, the divergence constraint on each element of the mesh is strongly guaranteed, see [6]. This provides us better theoretical convergence of the method.

This paper presents the numerical realization and comparison of numerical results for both TH and SV finite elements by using an in-house solver written in C language. The benchmark problem of nonstationary flow around the vibrating cylinder is chosen and the numerical results are compared with the reference data [1].

2. Governing equation

The mathematical model that describes the fluid-structure interaction consists of movement of the rigid structure (i.e. described by ordinary differential equations) and incompressible Navier-Stokes equations in the Eulerian-Lagrangian (ALE) formulation.

2.1. Incompressible fluid flow

Let us assume a computation fluid domain $\Omega_t \subset \mathbb{R}^2$ to be bounded and polygonal at any time $t \in (0,T)$. Furthermore, its boundary $\partial\Omega$ is assumed to be continuous Lipschitz boundary formed of three disjoint parts Γ_D, Γ_O and Γ_{W_t} (i.e. $\partial\Omega = \Gamma_D \cup \Gamma_O \cup \Gamma_{W_t}$). Flow in the domain Ω_t is described by incompressible Navier-Stokes equations in the ALE formulation. The ALE method is based on ALE mapping A_t which maps the reference domain configuration Ω_0 into the actual domain Ω_t

$$A_t : \Omega_{\text{ref}} \to \Omega_t, \quad X \mapsto x(X,t) = A_t(X), \quad x \in \Omega_{\text{ref}},\ t \in (0,T).$$

The ALE mapping is chosen in order to map reference position of the interface Γ_{W_0} into Γ_{W_t} whose position is defined by the motion of the cylinder, and the positions of boundaries Γ_D and Γ_O are static and they are not dependent on time, for more information see [13].

The Navier-Stokes equations in the ALE formulation for unknown velocity $\mathbf{u}(x,t)\colon \Omega_t \to \mathbb{R}^2$ with components $\mathbf{u} = (u,v)^T$ and the kinematic pressure $p(x,t)\colon \Omega_t \to \mathbb{R}$ read

$$\begin{aligned} \frac{D^A}{Dt}\mathbf{u} + [(\mathbf{u}-\mathbf{w})\cdot\boldsymbol{\nabla}]\mathbf{u} - \nu\boldsymbol{\Delta}\mathbf{u} + \boldsymbol{\nabla}p &= 0 \quad \text{in } \Omega_t, t \in (0,T], \\ \boldsymbol{\nabla}\cdot\mathbf{u} &= 0 \quad \text{in } \Omega_t, t \in (0,T], \end{aligned} \tag{1}$$

where $\frac{D^A}{Dt}$ is the ALE derivative, $\mathbf{w} = \partial A^t/\partial t$ is the domain velocity, see [13] and ν means the kinematic viscosity. We consider the following boundary conditions

$$\mathbf{u}(x,t) = \mathbf{g}(x,t) \quad \text{on } \Gamma_D \times (0,T], \tag{2}$$

$$\mathbf{u}(x,t) = \mathbf{w}(x,t) \quad \text{on } \Gamma_{W_t},\ t \in (0,T], \tag{3}$$

$$-(p - p_{\text{ref}})\mathbf{n} + \nu \frac{\partial \mathbf{u}}{\partial \mathbf{n}} = 0 \quad \text{on } \Gamma_O \times (0,T], \tag{4}$$

where $\mathbf{n}$ is the unit outward normal vector to $\partial\Omega$ and p_{ref} is a reference pressure value at the outlet. Condition (2) is used at the inlet. Furthermore, on the surface of the cylinder, the continuity of velocities is prescribed between the cylinder motion and the airflow. At the outlet, there is the condition (4) which is the so-called do-nothing condition, for more information see [5]. Furthermore, the equations are supplied by an initial condition

$$\mathbf{u}(x,0) = \mathbf{u}^0(x) \quad \text{in } \Omega_0.$$

2.2. Motion of cylinder

We consider the motion of the rigid cylinder with one degree of freedom. This means that the cylinder can move only in vertical directions, as in [1]. Its motion is described using the nondimensionless displacement Y governed by

$$\ddot{Y} + \left(\frac{4\pi\xi}{U_r}\right)\dot{Y} + \left(\frac{4\pi^2}{U_r^2}\right)Y = \frac{C_l}{2M^*}, \tag{5}$$

where $\ddot{Y}$, $\dot{Y}$ are the vertical acceleration and velocity of the rigid cylinder, ξ means the structural damping ratio, $U_r = \frac{U_\infty}{fD}$ represents the reduced velocity of the cylinder (where f denotes the natural frequency of the cylinder) and M^* is the reduced mass of the rigid cylinder ($M^* = \frac{m}{\rho D^2}$). The lift coefficient C_l is computed by

$$C_l = \frac{2}{\rho U_\infty^2 b D} F_l,$$

where b is the depth of the cylinder, U_∞ means free velocity, ρ expresses the density and F_l is the lift force acting on the cylinder of diameter D.

3. Numerical approximation of the Navier-Stokes equations

In order to approximate the problem (1), we start with time discretization. Here, the equidistant division $t_n = n\Delta t$ of the time interval $(0,T)$ is employed with a constant time step $\Delta t > 0$. Further, the velocity approximations at time step $t_n \in (0,T]$ are denoted by

$$\mathbf{u}^n(x) \approx \mathbf{u}(x,t_n) \quad \text{for } x \in \Omega_{t_n},$$

and similarly the pressure approximations are denoted as

$$p^n(x) \approx p(x,t_n) \quad \text{for } x \in \Omega_{t_n}.$$

The domain velocity is at the time instant t_{n+1} approximated by $\mathbf{w}^{n+1}(x) \approx \mathbf{w}(x, t_{n+1})$. The ALE derivative is approximated by implicit Euler (BDF) and we get

$$\begin{aligned} \frac{\mathbf{u}^{n+1} - \tilde{\mathbf{u}}^n}{\Delta t} + ((\mathbf{u}^{n+1} - \mathbf{w}^{n+1}) \cdot \boldsymbol{\nabla})\mathbf{u}^{n+1} - \nu \boldsymbol{\Delta} \mathbf{u}^{n+1} + \boldsymbol{\nabla} p^{n+1} &= 0, \\ \boldsymbol{\nabla} \cdot \mathbf{u}^{n+1} &= 0, \end{aligned} \tag{6}$$

where by $\tilde{\mathbf{u}}^n$ we denote the velocity from time level t^n defined in Ω_{t_n} transformed to $\Omega_{t_{n+1}}$, that is $\tilde{\mathbf{u}}^i := \mathbf{u}^i \circ A_{t_i} \circ A_{t_{n+1}}^{-1}$. Equations (6) are equipped with boundary conditions (2–4).

3.1. Space discretization

For the discretization of problem (6) by using the finite element method, a weak formulation of problem (6) is introduced. First, assuming the fixed time instant t_{n+1}, the simplified notation $\mathbf{u} := \mathbf{u}^{n+1}$, $\mathbf{w} := \mathbf{w}^{n+1}$, $p := p^{n+1}$ and $\Omega := \Omega_{t_{n+1}}$ are considered. Then we define the velocity test space $\boldsymbol{\mathcal{V}}$ and the pressure test space $\mathcal{Q}$ as

$$\boldsymbol{\mathcal{V}} = \left\{ \boldsymbol{\varphi} \in \mathbf{H}^1(\Omega) \colon \boldsymbol{\varphi}(x) = 0 \quad \forall x \in \Gamma_D \cup \Gamma_W \right\},$$

$$\mathcal{Q} = L^2(\Omega),$$

where $\mathbf{H}^1(\Omega) = [H^1(\Omega)]^2$ is the vector Sobolev space and $L^2(\Omega)$ is the Lebesgue space, see [10].

Now, we take a function $\mathbf{v} \in \boldsymbol{\mathcal{V}}$, multiply first of equations (6) and take an arbitrary $q \in \mathcal{Q}$, multiply second of equations (6) by it, integrate over the domain Ω and apply Green's theorem to the pressure gradient $(\boldsymbol{\nabla} p)$ and the viscous term $(-\nu \boldsymbol{\Delta} \mathbf{u})$. Further, the boundary conditions are used. Then the weak formulation reads: Find $\mathbf{u} \in \mathbf{g} + \boldsymbol{\mathcal{V}}$ and $p \in \mathcal{Q}$ such that the equations

$$\frac{1}{\Delta t}(\mathbf{u}, \mathbf{v})_\Omega + \nu(\boldsymbol{\nabla}\mathbf{u}, \boldsymbol{\nabla}\mathbf{v})_\Omega c(\mathbf{u} - \mathbf{w}, \mathbf{u}, \mathbf{v}) - (p, \boldsymbol{\nabla} \cdot \mathbf{v})_\Omega = \frac{1}{\Delta t}(\tilde{\mathbf{u}}^n, \mathbf{v})_\Omega, \tag{7}$$

$$(\boldsymbol{\nabla} \cdot \mathbf{u}, q)_\Omega = 0, \tag{8}$$

hold for any $\mathbf{v} \in \boldsymbol{\mathcal{V}}$ and $q \in \mathcal{Q}$. In these equations, $(\mathbf{u}, \mathbf{v})_\Omega = \int_\Omega \mathbf{u} \cdot \mathbf{v} \mathrm{d}x$ means the scalar product in $\mathbf{L}^2(\Omega)$ and $c(\mathbf{u}, \mathbf{v}, \mathbf{z})$ denotes the trilinear form. This form is defined by $c(\mathbf{u}, \mathbf{v}, \mathbf{z}) = \int_\Omega ((\mathbf{u} \cdot \boldsymbol{\nabla})\mathbf{v}) \cdot \mathbf{z} \mathrm{d}x$ for any $\mathbf{u}, \mathbf{v}, \mathbf{z} \in \boldsymbol{\mathcal{V}}$, for more details see [7].

For the reason of using the finite element method, we define an admissible triangulation τ_h of the domain Ω, see [4]. Now, we assume that the finite element subspaces $\boldsymbol{\mathcal{V}}_h \subset \boldsymbol{\mathcal{V}}$ and $\mathcal{Q}_h \subset \mathcal{Q}$ are approximations of the spaces $\boldsymbol{\mathcal{V}}$ and $\mathcal{Q}$ defined over the triangulation τ_h. These spaces are formed by piecewise polynomial functions. The discrete problem of problem (7) is as follows: Find $\mathbf{u}_h \in \mathbf{g}_h + \boldsymbol{\mathcal{V}}_h$ and $p_h \in \mathcal{Q}_h$ such that equations

$$\frac{1}{\Delta t}(\mathbf{u}_h, \mathbf{v}_h)_\Omega + \nu(\boldsymbol{\nabla}\mathbf{u}_h, \boldsymbol{\nabla}\mathbf{v}_h)_\Omega + c(\mathbf{u}_h - \mathbf{w}_h, \mathbf{u}_h, \mathbf{v}_h) - (p_h, \boldsymbol{\nabla} \cdot \mathbf{v}_h)_\Omega = \frac{1}{\Delta t}(\tilde{\mathbf{u}}_h^n, \mathbf{v}_h)_\Omega,$$

$$(\boldsymbol{\nabla} \cdot \mathbf{u}_h, q_h)_\Omega = 0, \tag{9}$$

hold for any $\mathbf{v}_h \in \boldsymbol{\mathcal{V}}_h$ and $q_h \in \mathcal{Q}_h$. To guarantee stability of the scheme, the couple $\boldsymbol{\mathcal{V}}_h$, $\mathcal{Q}_h$ should satisfy the BB condition, see [7]. In this paper, the well-known Taylor-Hood element and Scott-Vogelius element are used.

Taylor-Hood (P_2/P_1) finite element uses quadratic velocities and linear pressures, i.e. the spaces are defined by

$$\begin{aligned}\boldsymbol{\mathcal{V}}_h =&\left\{\boldsymbol{\varphi} \in \mathbf{C}(\overline{\Omega})\colon (\boldsymbol{\varphi}\big|_K \in P_2(K),\ \forall K \in \tau_h)\right\} \cap \boldsymbol{\mathcal{V}},\\ \mathcal{Q}_h =&\left\{\varphi \in C(\overline{\Omega})\colon (\varphi\big|_K \in P_1(K), \forall K \in \tau_h)\right\}.\end{aligned} \tag{10}$$

Velocity and pressure functions are continuous in the domain Ω, however, the element satisfies the continuity equation only discretely. This is the reason why we use the Scott-Vogelius P_2/P_1^{disc} element, which strongly guarantees divergence-free velocity on each element, see [3].

It has the same space $\boldsymbol{\mathcal{V}}_h$ (10) for velocity as TH element, whereas for the pressure p_h the linear but discontinuous functions are used, i.e.

$$\mathcal{Q}_h^{\text{disc}} = \left\{\varphi\colon \overline{\Omega} \to \mathbb{R}\colon (\varphi\big|_K \in P_1(K), \forall K \in \tau_h)\right\}.$$

In order to satisfy the BB condition, element is constructed over the barycentric refined mesh created from the given regular mesh, see [3]. For both cases the velocity and the pressure can be solved together as both couples satisfy BB condition.

So, the base $\boldsymbol{\Phi}_1, \ldots, \boldsymbol{\Phi}_{N_u}$ of the space $\boldsymbol{\mathcal{V}}_h$, where $N_u = \dim(\boldsymbol{\mathcal{V}}_h)$ is chosen. In addition, a base of the pressure space $\mathcal{Q}_h$ is defined by $\theta_1, \ldots, \theta_{N_p} \in \mathcal{Q}_h$, where $N_p = \dim(\mathcal{Q}_h)$. The approximation of the velocity $\mathbf{u}_h$ can be expressed as a combination of the basis functions of the space $\boldsymbol{\mathcal{V}}_h$

$$\mathbf{u}_h = \sum_{j=1}^{N_u} \alpha_j \boldsymbol{\Phi}_j. \tag{11}$$

and approximation of pressure p_h as a linear combination of the base of space $\mathcal{Q}_h$

$$p_h = \sum_{j=1}^{N_p} \beta_j \theta_j. \tag{12}$$

Equations (11) and (12) are now used in equations (9). Also, the test functions $\mathbf{v}_h$ and q_h in equation (9) are expressed as $\mathbf{v}_h = \boldsymbol{\Phi}_i$, for $i = 1, \ldots, N_u$ and $q_h = \theta_i$, for $i = 1, \ldots, N_p$. Then the system of nonlinear equations is obtained

$$\begin{pmatrix} \frac{1}{\Delta t}\mathbf{M} + \mathbf{A}(\boldsymbol{\alpha}) & \mathbf{B} \\ -\mathbf{B}^T & 0 \end{pmatrix} \begin{pmatrix} \boldsymbol{\alpha} \\ \boldsymbol{\beta} \end{pmatrix} = \begin{pmatrix} \mathbf{f} + \frac{1}{\Delta t}\mathbf{M}\tilde{\mathbf{u}}_h^n \\ 0 \end{pmatrix}, \tag{13}$$

where $\mathbf{M}$ denotes the mass matrix (which depends on the mesh, so it is different in each time step due to ALE formulation), $\mathbf{A}(\boldsymbol{\alpha})$ represents discretization of the nonlinear convective and the viscous terms, $\mathbf{B}$ corresponds to the discrete gradient

and $\mathbf{B}^T$ is the discrete divergence operator. Equations (13) is a system of nonlinear equations which is further to be linearized before it can be solved, see e.g. [9]. In this article the linearization is taken from previous time instant

$$c(\mathbf{u}_h^{n+1}, \mathbf{u}_h^{n+1}, \mathbf{v}_h^{n+1}) \approx c(\mathbf{u}_h^{n}, \mathbf{u}_h^{n+1}, \mathbf{v}_h^{n+1}).$$

Due to this linearization, there is a restriction on the choice of the time step, for more information see [9]. The linearized system of equations can be solved by some iterative methods e.g. GMRES, see [8] or a direct solver such as UMFPACK, MUMPS, MKL, see [11].

4. Numerical results

The benchmark problem of the flow around a movable cylinder [1] is regarded. The numerical results obtained by TH and SV elements are compared to each other and to the reference data. For the numerical solution of the cylinder motion given by equation (5), the Runge-Kutta method of 4th order was used.

The domain Ω_t is shown in Fig. 1 in its initial state. The cylinder has a radius $r = 0.5$ and its center is located at $[x, y] = [19, 20]$. The Dirichlet boundary condition is prescribed ($\mathbf{g} = (1, 0)$) at the inlet $\Gamma_{D,1}$ and at the wall $\Gamma_{D,2}$ zero velocity is given. At the cylinder surface Γ_{W_t} is used Dirichlet boundary condition of the form $\mathbf{u} = \mathbf{w}$. The problem is solved on meshes which are different for each considered finite element. Due to the discontinuity of the SV element, the number of unknowns is much higher than for the TH element. In order to compare both elements, meshes providing a similar number of unknowns are used. The first mesh A for TH leads to solving a system with 89519 unknowns, whereas the use of second mesh B for the SV element results to the system of 90798 unknowns for the SV element.

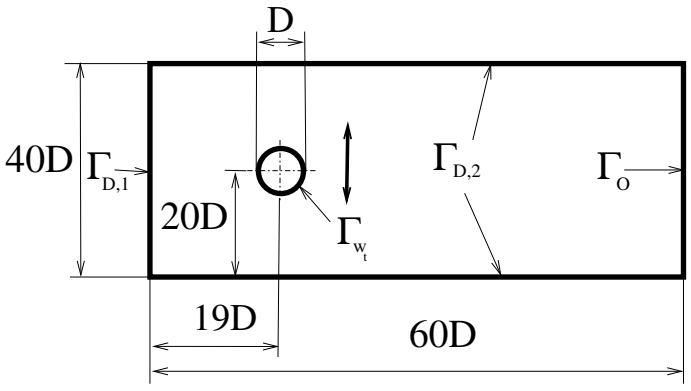

Figure 1: Fluid domain Ω_{ref} of the considered benchmark of flow around a movable cylinder, represented by interface Γ_{W_t}. Boundary Γ_D consists of two parts $\Gamma_{D,1}$ and $\Gamma_{D,2}$, where $\Gamma_{D,1}$ represents inlet and $\Gamma_{D,2}$ represents walls.

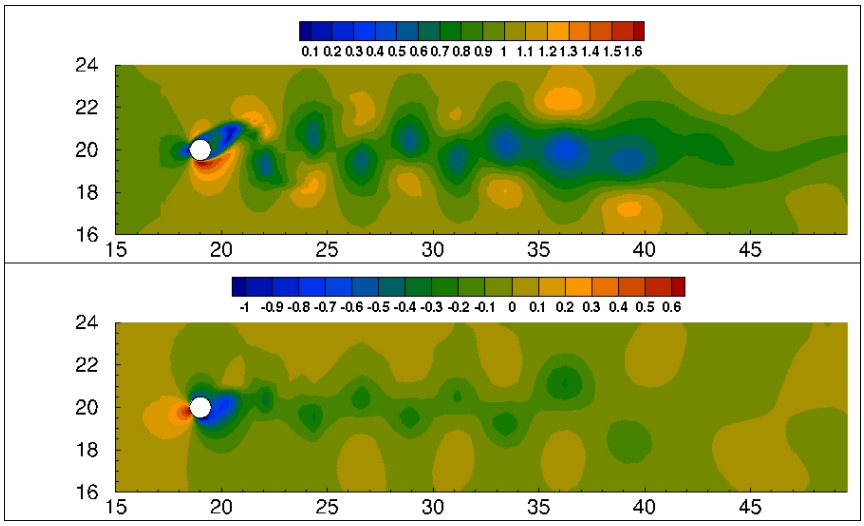

Figure 2: Velocity magnitude $||\mathbf{u}||_2$ (in the upper part) and the pressure p (in the lower part), for Re = 150 and $U_r = 3$ obtained by TH element.

The configuration of the problem is characterized by Reynolds number

$$Re = \frac{U_\infty D}{\nu}, \tag{14}$$

where the free stream velocity is $U_\infty = 1$ and ν expresses the kinematic viscosity. This setup provides us the same $Re = 150$ as the reference data [1]. The computations were done for several cases of different values of natural frequencies of the cylinder (realized by different values of U_r), in all cases the zero damping ratio is considered ($\xi = 0$) and reduced mass as $M^* = 2$, as in [1].

In Fig. 2, the velocity magnitude and pressure field is shown. The Von Karman vortex street is created behind the cylinder and the oscillations of the aerodynamic forces appear leading to the oscillations of the cylinder. For this case of $U_r = 3$, the SV and TH results are almost identical, see Fig. 3a). Further, it can be observed that if the frequency of Von Karman vortex street differs from the natural frequency of the cylinder, there is no resonance. On the other hand for the vortex shadding frequency close to the natural frequency of the cylinder the amplitudes of coefficients C_l, C_d and the amplitude of cylinder vibration are six times higher than for the previous case. Moreover, the peaks of the amplitudes occur in the same time. This phenomenon is called resonance. The resuts obtained by the SV element has slightly higher amplitudes of the displacement than the TH element.

The dependence of amplitude of cylinder oscilation on reduced velocity $U_r \in [3, 8]$ are shown in Fig. 4. The interval where we can see the resonance is the same as in the reference data [1] for both FE discretizations (i.e. $U_r \in [4, 7]$). The maximum amplitude is obtained for the case of $U_r = 4$. Then the amplitude decreases with increasing U_r, and finally for the case $U_r = 8$ there is no resonance.

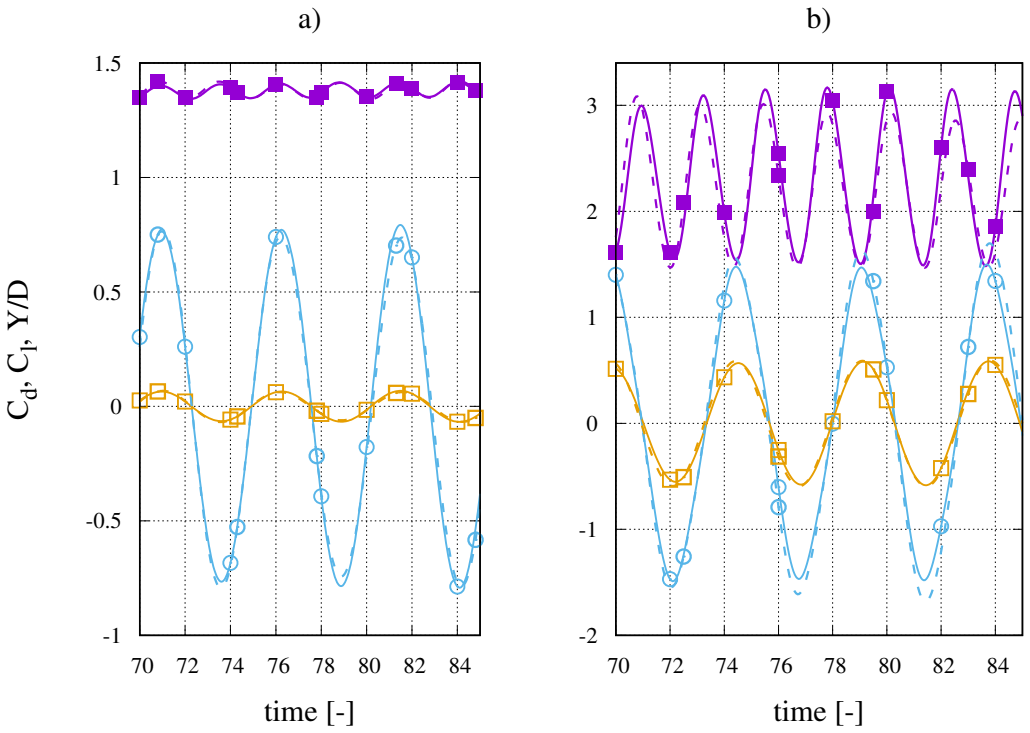

Figure 3: Comparison of lift C_L coefficient (line with empty circle), drag C_D coefficient (line with full square) and position Y/D (line with empty square) over time solved by TH element (full line) and SV element (dashed line) for a) Reynolds number $Re = 150$, $U_r = 3$ and b) Reynolds number $Re = 150$, $U_r = 4$.

5. Conclusion

In this article, the numerical approximation of the interaction of incompressible fluid flow with a movable rigid cylinder is performed. For the fluid flow description the incompressible Navier-Stokes equations in the ALE formulation is used and non-dimensional equation of cylinder motion is utilized. The coupled variables approach is chosen where the Taylor-Hood P_2/P_1 element and the Scott-Vogelius P_2/P_1^{disc} element are compared on the benchmark of movable cylinder in cross-flow, see [1].

The obtained numerical results agree well with the reference data, especially in the resonance occurrence for the considered interval of cylinder reduced velocity. As the maximum amplitudes obtained by the TH and SV elements are practically the same, it shows that the SV element performs well in this case in full agreement with the TH element, which can be considered here as the reference choice.

Although the SV element theoretically provides better results for the considered benchmark test, with similar number of unknowns the TH element has comparable results. The further advantages of the SV element is expected for higher Reynolds numbers, on what we will focus in our future work.

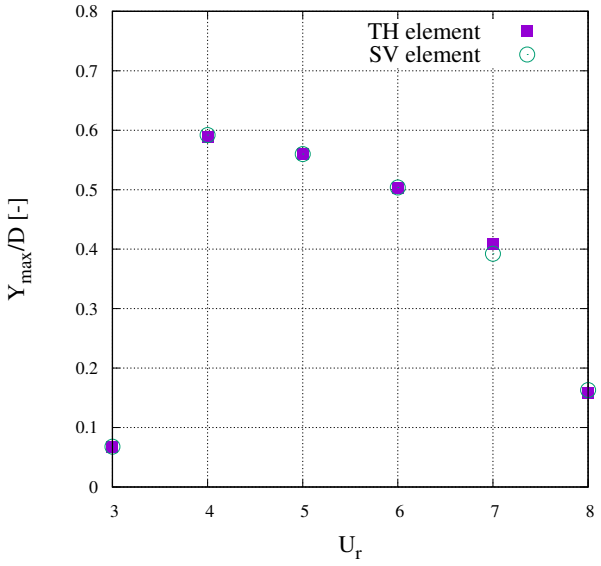

Figure 4: Comparison of maximum amplitudes for different reduced velocities U_r obtined by the TH and the SV elements for $Re = 150$ and $M^* = 2$.

Acknowledgements

Petr Sváček acknowledges the support from the EU Operational Programme Research, Development and Education, and from the Center of Advanced Aerospace Technology (CZ.02.1.01/0.0/0.0/16_019/0000826), Faculty of Mechanical Engineering, Czech Technical University in Prague. The authors also acknowledge the support by the Grant Agency of the Czech Technical University in Prague, grant No. SGS SGS22/148/OHK2/3T/12, and Karel Vacek has also been supported by the Czech Science Foundation (GAČR) project 22-01591S. The Institute of Mathematics of the Czech Academy of Sciences is supported by RVO:67985840.

References

[1] Ahn, H. T. and Kallinderis, Y.: Strongly coupled flow-structure interactions with a geometrically conservative ALE scheme on general hybrid meshes. Journal of Computational Physics **219** (2006), 671–696.

[2] Bao, Y., Huang, C., Zhou, D., Tu, J., and Han, Z.: Two-degree-of-freedom flow-induced vibrations on isolated and tandem cylinders with varying natural frequency ratios. Journal of Fluids and Structures **35** (2012), 50–75.

[3] Case, M. A., Ervin, V. J., Linke, A., and Rebholz, L. G.: A connection between Scott—Vogelius and grad-div stabilized Taylor—Hood FE approximations of the Navier—Stokes equations. SIAM Journal on Numerical Analysis **49** (2011), 1461–1481.

[4] Ciarlet, P. G.: *The Finite Element Method for Elliptic Problems*. Society for Industrial and Applied Mathematics, 2002.

[5] Feistauer, M. and Feistauer, M.: *Mathematical methods in fluid dynamics*. 67, Chapman and Hall/CRC, 1993.

[6] Gauger, N. R., Linke, A., and Schroeder, P. W.: On high-order pressure-robust space discretisations, their advantages for incompressible high Reynolds number generalised Beltrami flows and beyond. The SMAI journal of computational mathematics **5** (2019), 89–129.

[7] Girault, V. and Raviart, P.: *Finite Element Methods for Navier-Stokes Equations: Theory and Algorithms*. Computational Mathematics Series, Springer-Verlag, 1986.

[8] Gupta, P. K. and Pagalthivarthi, K. V.: Application of multifrontal and GMRES solvers for multi-size particulate flow in rotating channels. Progress in Computational Fluid Dynamics, an International Journal **7** (2007), 323–336.

[9] Karniadakis, G. and Sherwin, S.: *Spectral/hp Element Methods for Computational Fluid Dynamics: Second Edition*. Numerical Mathematics and Scientific Computation, OUP Oxford, 2013.

[10] Kufner, A., John, O., and Fučik, S.: *Function Spaces*. Mechanics: Analysis, Springer Netherlands, 1977.

[11] Raju, M. and Khaitan, S.: High performance computing of three-dimensional finite element codes on a 64-bit machine. Journal of Applied Fluid Mechanics **5** (2012).

[12] Sváček, P., Feistauer, M., and Horáček, J.: Numerical simulation of flow induced airfoil vibrations with large amplitudes. Journal of Fluids and Structures **23** (2007), 391–411.

[13] Takashi, N. and Hughes, T. J.: An arbitrary Lagrangian-Eulerian finite element method for interaction of fluid and a rigid body. Computer Methods in Applied Mechanics and Engineering **95** (1992), 115–138.